International Immunopharmacology 67 (2019) 366–371

Contents lists available at ScienceDirect

International Immunopharmacology

journal homepage: www.elsevier.com/locate/intimp

Preliminary report

Characterization of morphological changes of B16 melanoma cells under natural killer cell attack

Ji Sung Kim[a,1], Boyeong Kim[a,1], Hong Kyung Lee[a], Hyung Sook Kim[a], Eun Jae Park[a], Yeo Jin Choi[a], Gi Beom Ahn[a], Jieun Yun[b], Jin Tae Hong[a], Youngsoo Kim[a], Sang-Bae Han[a,*]

[a] College of Pharmacy, Chungbuk National University, Cheongju, Chungbuk 28160, Republic of Korea
[b] Department of Pharmaceutical Engineering, Cheongju University, Cheongju, Chungbuk 28503, Republic of Korea

ARTICLE INFO

Keywords:
Melanoma
NK cells
Writhing morphology
MYL9

ABSTRACT

Natural killer (NK) cell killing of melanoma cells involves perforin-mediated delivery of granzymes from NK cells to cancer cells; however, how melanoma cells die remains poorly characterized. Here, we examined the dying process of melanoma cells by using time-lapse imaging. Upon contact with NK cells, B16-F10 cells rounded and most of them showed membrane rupture (98 min); however, B16 parent cells showed writhing and delayed membrane rupture (235 min). This morphological difference depended on the expression levels of myosin regulatory light chain 9 (MYL9) but not activating ligands (CD112, CD155, Rae-1, and MULT-1), SPI, FasL, or PD-L1. Taken together, our data show that melanoma cells show two distinct types of morphological changes upon contact with NK cells and suggest that a strategy to decrease MYL9 expression by melanoma cells may improve the efficacy of NK cell–based immunotherapy.

1. Introduction

Melanoma remains the main cause of mortality in Caucasians and its incidence rate continuously increases in many countries [1,2]. Melanoma resistance to classical chemo- and radio-therapies and its high immunogenicity prompt the development of immunotherapies including T and NK cell therapy [3]. The susceptibility of melanoma to NK cells might be primarily determined by the expression levels of activating and inhibitory ligands on melanoma cells and their binding capacity to respective receptors on NK cells [4]. Melanoma cells express large amount of activating ligands, such as Rae-1, MULT-1, CD112, and CD155, which bind to activating receptors, such as NKG2D and DNAM-1, leading to effective NK cell activation [5]. Melanoma cells have low levels of the inhibitory ligand MHC-I, which increases melanoma susceptibility to NK cells [6].

NK cells use granule exocytosis to kill cancer cells, which involves perforin-mediated delivery of granzymes from NK cells to cancer cells [7,8]. Once inside the cancer cells, granzyme B, a member of serine protease family, activates caspase-3, which activates the serine/threonine kinase Rho-associated coiled coil–containing protein kinase (ROCK) I, an effector of the small GTPase Rho [9–11]. Activated ROCK I increases the phosphorylation of myosin regulatory light chain and thus stimulates actomyosin contraction, which is required for apoptotic membrane blebbing [12]. Ultimately, cancer cells under NK cell attack show rounding, shrinkage, and membrane rupture, which are classical morphological changes observed at the onset of apoptosis [12].

Although much has been learned about these morphological changes, a fundamental question of how melanoma cell death is induced by NK cells remains unanswered. Do all melanoma cell lines undergo the classical dying process? If not, is there another dying process? To address this simple issue, we examined the dying of B16 melanoma cell lines under NK cell attack by using time-lapse imaging. Our data show that B16 lines show two distinct types of morphological changes under NK cell attack depending on the expression level of myosin regulatory light chain 9 (MYL9).

2. Materials and methods

2.1. Mice and cells

C57BL/6 mice were purchased from Samtako (Gyeonggi, Korea). NK cells were isolated from the spleen by negative selection using an NK isolation kit (Miltenyi Biotec, Auburn, CA, USA). Purified NK cells were cultured in RPMI 1640 medium supplemented with 3000 U/ml

* Corresponding author at: 194-31, Osongsaengmyung-1, Heungdeok, Cheongju, Chungbuk 28160, Republic of Korea.
E-mail address: shan@chungbuk.ac.kr (S.-B. Han).
[1] These authors contributed equally to this work.

https://doi.org/10.1016/j.intimp.2018.12.037
Received 27 August 2018; Received in revised form 14 December 2018; Accepted 14 December 2018
Available online 21 December 2018
1567-5769/

recombinant human IL-2 (Bayer HealthCare Pharmaceuticals, Emeryville, CA, USA), 10% fetal bovine serum, 2 mM L-glutamine, 100 U/ml penicillin, 100 μg/ml streptomycin, and 50 μM 2-mercaptoethanol. Cell purity exceeded 90%. IL-2-activated NK cells were used from day 9 to 11 [13]. The parent B16 and its variant B16-F10 cell lines were provided by the Korea Research Institute of Bioscience and Biotechnology (Chungbuk, Korea) and maintained in DMEM medium containing 10% fetal bovine serum, 2 mM L-glutamine, 100 U/ml penicillin, and 100 μg/ml streptomycin. B16-F10 cells were more metastatic than B16 cells because they were selected by 10 successive passages of lung colonies with *in vivo–in vitro* selection based on the Fidler's method [14]. All animal studies were approved by the Chungbuk National University Animal Experimentation Ethics Committee and were carried out in accordance with the approved guidelines.

2.2. Flow cytometry

Cells were stained for 15 min at 4 °C with antibodies against mouse CD3, CD69, ICAM-1, H-2K^b, NK1.1, NKG2D (BD Biosciences, San Jose, CA, USA), DNAM-1, CD155, CD112, Ly49C/I (BioLegend, San Diego, CA, USA), LFA-1, Ly49A, KLRG-1, TIGIT, Rae-1, or MULT-1 (R&D Systems, Minneapolis, MN, USA) [15]. To analyze exocytosis, NK cells (1×10^5) were mixed with B16 or B16-F10 cells (1×10^5), centrifuged at 1000 rpm for 1 min, and incubated for 2 h at 37 °C in the presence of anti-CD107a–FITC antibody (BD Biosciences). The cells were then stained with anti-NK1.1–APC antibody. Cells were analyzed using a FACSCalibur flow cytometer (BD Biosciences) and the data were processed using Cell Quest Pro software (BD Biosciences).

2.3. Cytotoxicity assay

NK cells were incubated with target cells in 96-well plates at various effector-to-target cell ratios. After 4-h incubation, the plates were centrifuged and 100 μl of the supernatants was transferred to new 96-well plates. Target cell death was determined using LDH release assay (Takara, Shiga, Japan). The percentage of specific lysis was calculated from LDH content as follows: (experimental release–target spontaneous release–effector spontaneous release)/(target maximum release–target spontaneous release) × 100%.

2.4. RT-PCR

Total RNA from B16 and B16-F10 cells was isolated using TRIZOL Reagent (Life Technologies, Carlsbad, CA, USA). RNA was quantified using a spectrophotometer and cDNA was synthesized from 3 μg total RNA using an RT kit (Bioneer, Daejeon, Korea). The primer sequences were as follows: MYL9, sense, 5′-TCA GGC TTC ATC CAC GAG-3′, antisense, 5′-GGG CAG CTA AGA ACA GCT TAG-3′; ACTA2, sense, 5′-GTC CCA GAC ATC AGG GAG TAA-3′, antisense, 5′-TCG GAT ACT TCA GCG TCA GGA-3′; SPP1, sense, 5′-GCC GAG GTG ATA GCT TGG CTT AT-3′, antisense, 5′-ATG GCT GCC CCT TCC GTT GT-3′; β-actin, sense, 5′-TGG AAT CCT GTG GCA TCC ATG AAA C-3′, antisense 5′-TAA AAC GCA GCT CAG TAACAG TCC G-3′. PCR products were separated on 1% agarose gels and stained with 5 μg/ml ethidium bromide.

2.5. RNA interference

A double-stranded small interfering RNA (siRNA) oligonucleotide targeting MYL9 (GenBank accession number NM_172118), 5′-GAA GGG AUC UCU GAC CCU AdTdT-3′, was synthesized by Sigma-Aldrich (St. Louis, MO, USA). siRNAs against ACTA2 (GenBank accession number NM_007392), 5′-GCA UAC ACA CGU GCA UGG AdTdT-3′, and SPP1 (NM_001204201), 5′-CUC UUC CAA GCA AUU CCA AdTdT-3′, were synthesized by Bioneer (Daejeon, Korea). Each siRNA was transfected into B16 cells (25 pmol per well of a 6-well plate) using Lipofectamine RNAiMAX (Thermo Fisher Scientific, Waltham, MA, USA) following the manufacturer's instructions. Cells were incubated with the siRNA–lipid complex in growth medium without antibiotics for 24 or 48 h. Control cells were transfected with a negative control siRNA oligonucleotide at a matching concentration.

2.6. Time-lapse imaging

B16 cells were stained with 1 μM calcein acetoxymethyl ester (Calcein AM, Thermo Fisher Scientific) in serum-free medium for 30 min at 37 °C, and washed twice. B16 cells (5×10^4 cells/35 mm dish) were pre-cultured in serum-containing medium for 4 h at 37 °C and NK cells (1×10^5 cells/35 mm dish) were added to calcein AM–labeled target cells. Propidium iodide (PI, 2 μM) was added to the medium to stain dead cells. Time-lapse imaging was performed with a Biostation IM-Q microscope equipped with a 20× magnification objective (numeric aperture 0.5) in an environmental chamber kept at 37 °C and 5% CO_2 (Nikon Inc., Melville, NY, USA). Dishes were pre-incubated for 1 h in the chamber and images were acquired every 2 min for 8 h. PI-stained and calcein AM–leaking B16 cells were considered dead.

2.7. Statistics

Data represent the mean ± SEM of at least 3 independent experiments each performed in triplicate; p values were calculated using Student's t-test or one-way ANOVA in GraphPad Prism (GraphPad Prism Software, San Diego, CA, USA). For NK or target cell counts, p values were calculated using Mann–Whitney U test in GraphPad Prism software.

3. Results

3.1. B16 cells are resistant to NK cell killing

First, we examined the expression levels of cell surface molecules that affect NK cell cytotoxicity. IL-2-activated NK cells showed typical expression pattern of the activation receptors, such as NKG2D, NKp46, DNAM-1, and LFA-1, and the inhibitory receptors, such as Ly49A, Ly49C/I, and KLRG-1, as previously reported [3–5] (Fig. 1A). B16-F10 and B16 melanoma cells expressed similar levels of DNAM-1 ligands (CD155 and CD112), but did not express the MHC class I molecule H-2K^b, which binds to inhibitory receptors Ly49C and/or Ly49I (Fig. 1B). Only B16 cells expressed NKG2D ligands, such as Rae-1 and MULT-1. These data imply that NK cells could receive stronger activating signals from B16 than B16-F10 cells and kill B16 cells better than B16-F10 cells. However, NK cells degranulated similarly upon contacting B16-F10 and B16 cells for 1, 2, and 3 h (Fig. 1C). Unexpectedly, NK cells killed B16-F10 cells better than B16 cells (Fig. 1D). Recombinant perforin and granzyme B also killed B16-F10 cells better than B16 cells (Fig. 1E). These data suggest that B16-F10 cells are more sensitive to NK cell cytotoxicity than B16 cells, despite no expression of activating ligands (Rae-1 and MULT-1).

3.2. Resistance of B16 cells depends on MYL9 expression level

Next, we examined why B16 cells are resistant to NK cell cytotoxicity. To identify other factors involved in their susceptibility to NK cell–induced lysis, we analyzed gene expression profiles of B16 and B16-F10 cells using a cDNA microarray, which detected a total of 41,346 genes. The expression of 313 and 200 genes was increased and decreased by at least 4-fold in B16 cells relative to B16-F10 cells, respectively (Supplementary Fig. S1). KEGG pathway analysis showed that the differentially expressed genes were enriched mainly in the categories of vascular smooth muscle contraction and extracellular matrix–receptor interaction (Supplementary Table 1). In particular, the expression levels of ACTA2, MYL9, and SPP1 in B16 cells were much

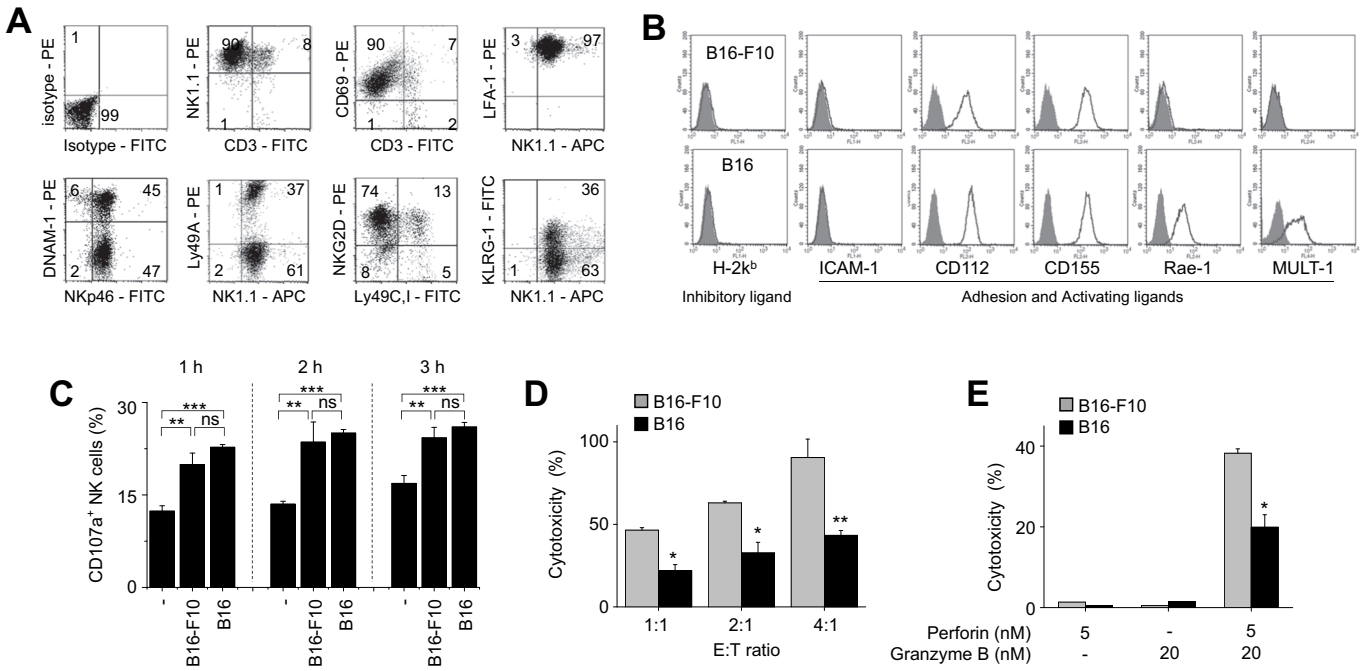

Fig. 1. B16 melanoma cells are resistant to NK cell killing.
(A) Representative phenotypes of NK cells (n = 5). (B) Representative phenotypes of B16-F10 and B16 parent cells (n = 5). Cells were stained with IgG isotype control (filled histogram) and various Abs indicated in Figs (open histogram). (C) To analyze exocytosis, NK cells were co-cultured with B16-F10 or B16 cells for 1–3 h in the presence of anti-CD107a–FITC antibody. CD107 expression level on NK cells was determined using flow cytometry (n = 3). $^{**}p < 0.01$; $^{***}p < 0.001$; ns, not significant (one-way ANOVA). (D) Cytotoxicity of NK cells against B16-F10 and B16 cells was determined by the LDH assay (n = 3). $^{*}p < 0.05$; $^{**}p < 0.01$ (Student's *t*-test). (E) Cytotoxicity of recombinant perforin and/or granzyme B against B16-F10 and B16 cells (n = 3). $^{*}p < 0.05$ (Student's *t*-test).

higher (53.5-, 10.1-, and 36.9-fold, respectively) than in B16-F10 cells (Supplementary Table 2). Thus, we examined their role in B16 cell lysis by NK cells by using siRNAs. NK cells killed B16 cells transfected with MYL9 siRNA better than B16 cells transfected with negative-control siRNA (Fig. 2A). Knockdown of MYL9 mRNA level in B16 cells transfected with siRNA was confirmed by RT-PCR (Fig. 2A). ACTA2 and SPP1 siRNA did not affect the susceptibility of B16 cells to NK cell cytotoxicity (Fig. 2B and C). Next, we examined the effects of other well-known factors affecting NK cell cytotoxicity against cancer cells. Serine protease inhibitor (SPI) inhibits granzyme B [16,17], but SPI siRNA did not increase B16 cell killing by NK cells (Fig. 2D). Both melanoma cell lines did not express Fas ligand (FasL; Fig. 2E) and expressed similar levels of programmed death ligand 1 (PD-L1; Fig. 2F), which are well-known ligands to inhibit NK cells [18,19]. NK cells degranulated similarly upon contacting B16 cells transfected with negative control siRNA or MYL9 siRNA (Fig. 2G). Overall, these data suggest that the resistance of B16 cells to NK cells depends on MYL9, but not other proteins we tested.

3.3. Contact dynamics between B16 cells and NK cells

Next, we confirmed the difference in susceptibility of B16 and B16-F10 cells to NK cells at the single-cell level. We mixed NK cells with calcein AM–stained B16-F10 cells (Supplementary movie S1), B16 cells (Supplementary movie S2), or B16 cells transfected with MYL9 siRNA (Supplementary movie S3) and imaged them by using time-lapse microscopy. Representative images collected at 2-h intervals for 8 h are shown in Fig. 3A. NK cells killed more B16-F10 cells than B16 cells (Fig. 3B). Transfection of B16 cells with MYL9 siRNA increased their killing by NK cells (Fig. 3B). However, the frequency of NK cell contacts with the three kinds of target cells was similar, 1 or 2 contacts per cancer cell over the observation period (Fig. 3C). Next, we analyzed the migration behavior of NK cells around the target cells. NK cells showed similar migration speed (5 μm/min, Fig. 3D), similar track length (Fig. 3E), similar track straightness (Fig. 3F), and similar mean square displacement (Fig. 3G) in all cases. Overall, these data suggest that MYL9 affects target cell susceptibility to NK cells, but not the behavior of NK cells.

3.4. B16 cells show writhing morphological changes

Next, we analyzed the dying process of melanoma cells. Upon contact with NK cells, B16-F10 cells showed the classical dying process: they rapidly rounded, detached from the substratum, and were stained with PI within on average 98 min (Supplementary movie S4, Fig. 4A; referred to hereafter as rounding-type cell death). After 8 h of co-culture, 60% of B16-F10 cells were stained with PI (Fig. 3B) and most of the PI-positive cells (88%) underwent rounding-type cell death (Fig. 4C and D).

In contrast, B16 cells displayed distinct morphological changes: upon contact with NK cells, B16 cells showed writhing and worm-like morphology and were stained with PI within on average 235 min, which was much longer than in the case of B16-F10 cells (Supplementary movie S5, Fig. 4B; referred to hereafter as writhing-type cell death). After 8 h of co-culture, 30% of B16 cells were stained with PI (Fig. 3B) and most of the dying cells (73%) underwent writhing-type cell death (Fig. 4C and D). Similar to B16-F10 cells, most of the B16 cells transfected with MYL9 siRNA underwent rounding-type cell death (Fig. 4C and D). Overall, these data suggest that melanoma cells highly expressing MYL9 show writhing-type cell death, which is distinct from rounding-type cell death.

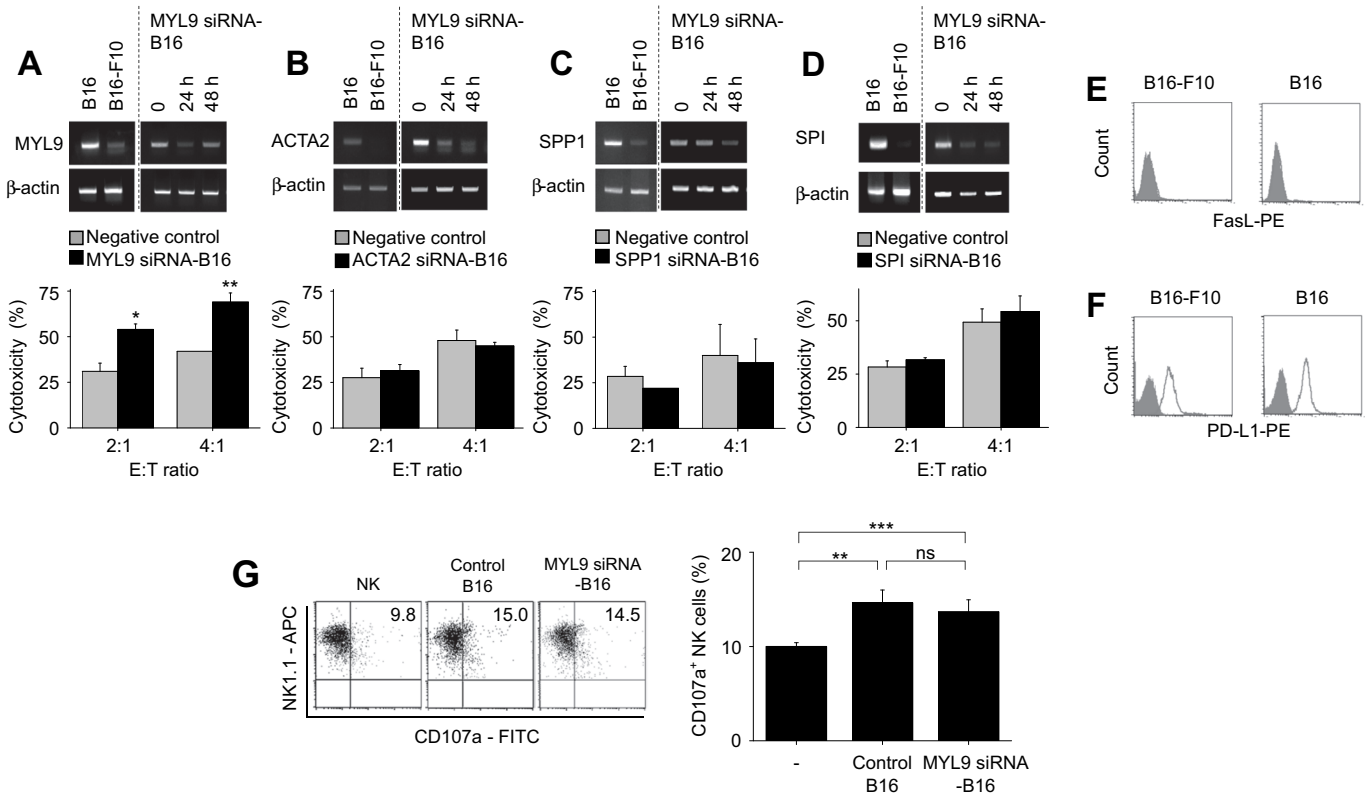

Fig. 2. The resistance of B16 cells depends on MYL9 expression level.
(A–D) NK cell cytotoxicity to B16 cells transfected with MYL9 siRNA (A). ACTA siRNA (B), SPP siRNA (C), and SPI siRNA (D). MYL9 expression level in melanoma cells was estimated by RT-PCR. $*p < 0.05$; $**p < 0.01$ (Student's *t*-test). (E, F) Expression levels of FasL (E) and PD-L1 (F) on melanoma cells were determined by flow cytometry. Cells were stained with IgG isotype control (filled histogram) and anti-FasL or anti-PD-L1 (open histogram). (G) To analyze exocytosis, NK cells were co-cultured with B16 cells transfected with negative control siRNA or MYL9 siRNA for 2 h in the presence of anti-CD107a–FITC antibody. CD107 expression level on NK cells was determined using flow cytometry (n = 3). $**p < 0.01$; $***p < 0.001$; ns, not significant (one-way ANOVA).

4. Discussion

Our study provides several insights into the dying process of melanoma cells attacked by NK cells. We found that, upon contact with NK cells, melanoma cells undergo two distinct types of morphological changes: rounding and writhing. NK cell–sensitive melanoma cells show rounding and die within 98 min, but NK cell–resistant melanoma cells show writhing and die within 235 min. This difference might be due to the difference in the expression levels of MYL9, but not activating ligands and other proteins, such as SPI, PD-L1, and FasL.

Our study extends the previous data on the morphological changes of cancer cells contacting NK cells. Although wild-type NK cells induce classical rounding-type cell death, NK cells from granzyme B–deficient mice show slow writhing-type cell death [7]. Granzyme B induces rapid rounding-type cell death, which includes degradation of cytoskeleton proteins, such as actin and tubulin, induction of mitochondrial dysfunction, reactive oxygen species generation, and caspase-3 activation [20]. In contrast, granzyme A induces slow writhing-type cell death, similar to that in B16 cells in our study, which does not involve mitochondrial damage or caspase-3 activation [7]. These previous data suggest that NK cells might be able to decide the type of cancer cell death. In contrast, our data suggest that cancer cells can determine the type of their death: melanoma cells with low MYL9 expression will die with rounding, but those with high MYL9 expression will slowly die with writhing.

The main question posed in this study is how MYL9 affects the morphological changes and susceptibility of melanoma cells to NK cells. As cells transform from non-malignant to cancerous, their cytoskeletal structure changes from an organized to an irregular network, suggesting the close relationship between cytoskeletal structure and cancer progression [21]. Cell stiffness is regulated by a dynamic network of structural, cross-linking, and signaling molecules [22]. As one of the structural proteins, non-muscle myosin II is an actin-binding protein composed of three pairs of polypeptides: two heavy chains, two regulatory light chains, and two essential light chains [23]. The action of non-muscle myosin II is regulated by the regulatory light chains, which are encoded by the MYL9 gene, which is known to affect cell stiffness [23]. Our data might suggest that B16 melanoma highly expressing MYL9 might be relatively stiff, which renders them to be more resistant to NK cell killing. Interestingly, MYL9 increases adhesion, migration, and metastasis of several cancer cell types. Cancer patients with high MYL9 expression in esophageal squamous cell carcinoma have poor overall survival and recurrence-free survival [24]. Medjkane et al. reported that MYL9 depletion in MDA-MB-231 breast cancer cells and B16-F2 melanoma cells with siRNA reduced invasion, adhesion, and lung metastasis and MYL9 overexpression in B16-F0 cells increased lung metastasis in mice [25]. Based on the previous and our data, we can presume that MYL9 might render B16 melanoma cells to evade NK cell attack during the circulation in blood and might render them to migrate and localize well in the secondary metastatic tissues. Yet, it is unclear whether MYL9 has dual functions, since all data are originated from different types of cancer cells. To address this issue, further studies are required to examine how MYL9 affects the susceptibility to NK cell cytotoxicity and metastasis of a type of cancer cells.

It is becoming clear that cancer cells might escape NK cell–induced killing by down-regulating activating ligands and up-regulating inhibitory ligands [26]. In addition, suppression of NK cells by soluble factors, such as prostaglandin E_2 and indoleamine 2,3-dioxygenase, which are secreted by cancer cells and suppressive immune cells in the tumor microenvironment, contributes to cancer escape from NK cells

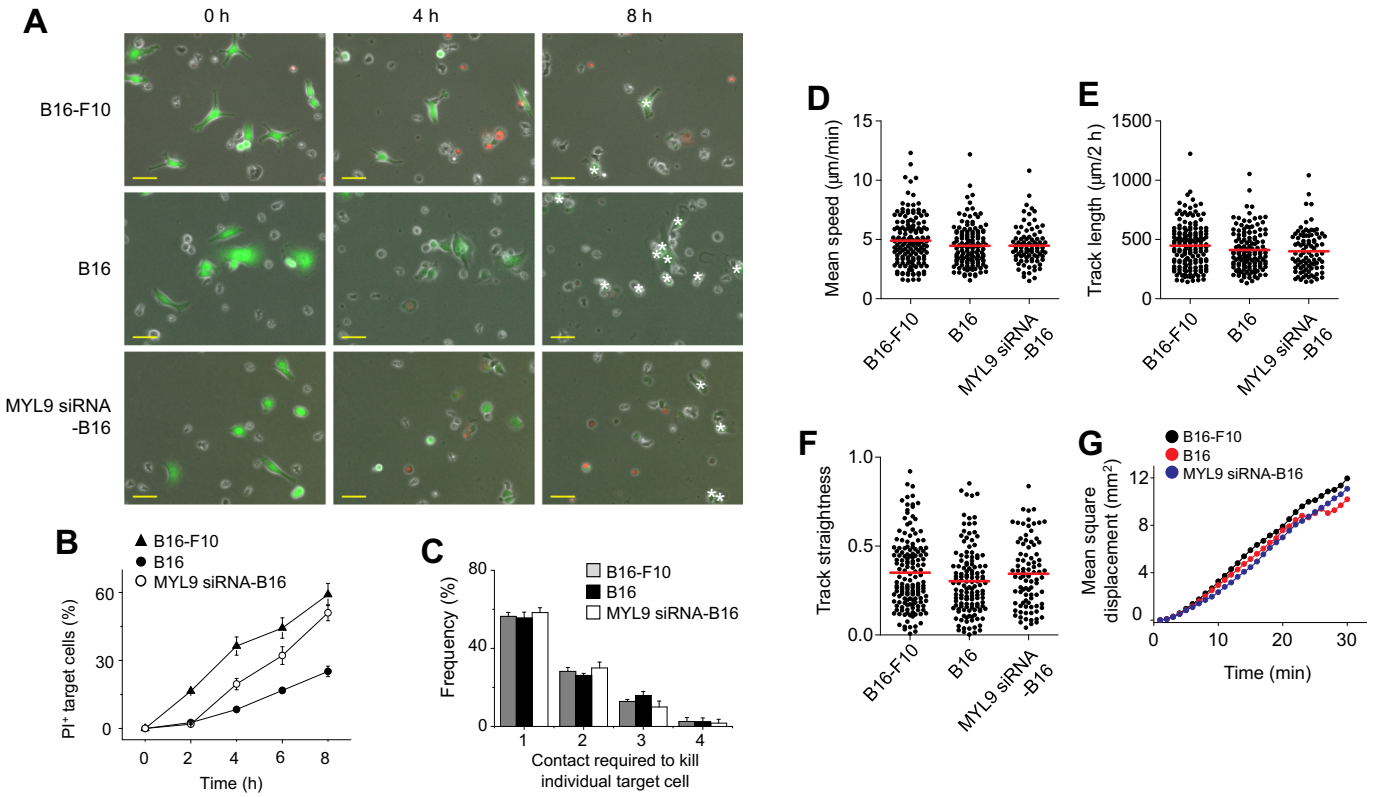

Fig. 3. Contact dynamics between NK cells and melanoma cells.
(A) Unstained NK cells and calcein AM–stained melanoma cells were imaged every 2 min for 8 h. Representative images of NK cells co-cultured with B16-F10 (top), B16 (middle), or B16 cells transfected with MYL9 siRNA (bottom) are shown. White asterisks indicate viable target cells. (B) Percentage of PI^+ target cells was calculated every 2 h for 8 h (from six movies from three independent experiments). (C) The number of contacts with NK cells required to kill individual target cells was calculated for 8–h co-culture. (D) Mean speed of NK cells (n = 153, 134, and 91 from the left). (E) Track length of NK cells that migrated for 2 h. (F) Track straightness of NK cells. (G) Mean square displacement of NK cells (n = 153 for B16-F10, 134 for B16, and 91 for B16-siRNA).

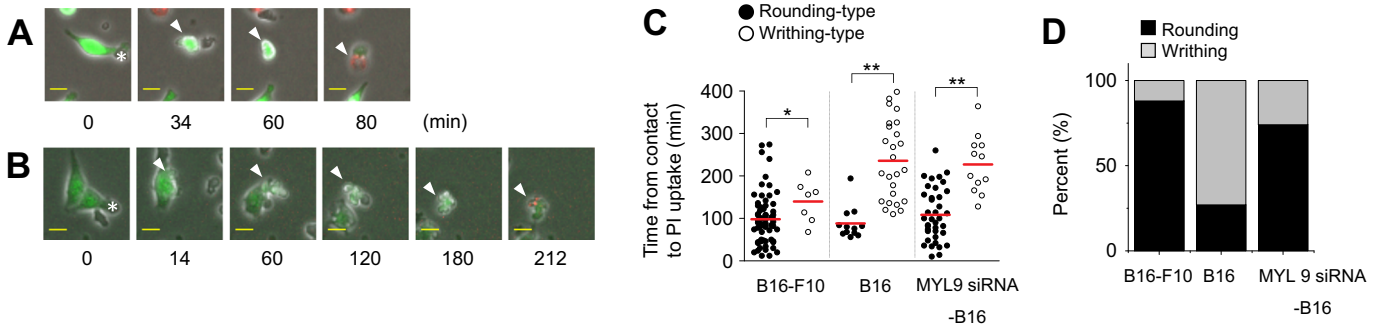

Fig. 4. B16 cells show distinct morphological changes upon contact with NK cells.
(A, B) Representative images of the dying process of (A) B16-F10 cells and (B) B16 cells. Asterisks, NK cells; arrowheads, melanoma cells. (C) Time from contact to PI uptake (n = 69, 7, 12, 25, 38, and 12 from the left). *$p < 0.05$; **$p < 0.01$ (Mann–Whitney *U* test). (D) Percentage of rounding- or writhing-type cell death.

[27]. High expression of SPI, which is detected in cervical carcinoma as well as lung and prostate cancer cells, is another escape mechanism from granzyme B–mediated apoptosis induced by NK cells [16,17]. Overexpression of PD-L1 and FasL on the surface of cancer cells inhibits NK cells *via* binding to PD-1 and Fas receptors on NK cells, respectively [18,19]. Our data provide evidence that melanoma cell escape from NK cells might be independent from the expression levels of activating ligands (Rae-1, MULT-1, CD155, and CD112), SPI, FasL, and PD-L1.

In summary, our data show that MYL9 plays an important role in determination of melanoma cell susceptibility to NK cells and that the phenotypic heterogeneity of melanoma cells upon contact with NK cells might be a good prognostic biomarker to predict their susceptibility to NK cells. In addition, our data suggest that a strategy to decrease MYL9 expression by melanoma cells may improve the efficacy of NK cell–-based immunotherapy. However, further study will be required to clarify the molecular mechanisms of the effect of MYL9 on melanoma cell death. It will be interesting to determine the relationship between MYL9 and granzyme A, which both are related with writhing morphological changes in cancer cells. It will also be interesting to examine whether MYL9 affects cytochrome *c* release from mitochondria, reactive oxygen species production, mitochondrial transmembrane potential loss, and caspase activation, which are classical events in cancer cells contacting NK cells [7].

Supplementary data to this article can be found online at https://doi.org/10.1016/j.intimp.2018.12.037.

Acknowledgement

This study was supported by grants funded by the Korean Government (NRF-2017R1A5A2015541 and NRF-2017M3A9B4050336).

Conflicts of interest

No potential conflicts of interest were disclosed.

References

[1] H. Tsao, M.B. Atkins, A.J. Sober, Management of cutaneous melanoma, N. Engl. J. Med. 351 (10) (2004) 998–1012.
[2] F. Erdmann, J. Lortet-Tieulent, J. Schuz, H. Zeeb, R. Greinert, E.W. Breitbart, F. Bray, International trends in the incidence of malignant melanoma 1953–2008—are recent generations at higher or lower risk? Int. J. Cancer 132 (2) (2013) 385–400.
[3] R. Tarazona, E. Duran, R. Solana, Natural killer cell recognition of melanoma: new clues for a more effective immunotherapy, Front. Immunol. 6 (2015) 649.
[4] K.M. Mirjacic Martinovic, N. Babovic, R.R. Dzodic, V.B. Jurisic, N.T. Tanic, G.M. Konjevic, Decreased expression of NKG2D, NKp46, DNAM-1 receptors, and intracellular perforin and STAT-1 effector molecules in NK cells and their dim and bright subsets in metastatic melanoma patients, Melanoma Res. 24 (4) (2014) 295–304.
[5] J.M. Chauvin, O. Pagliano, J. Fourcade, Z. Sun, H. Wang, C. Sander, J.M. Kirkwood, T.H. Chen, M. Maurer, A.J. Korman, H.M. Zarour, TIGIT and PD-1 impair tumor antigen-specific CD8(+) T cells in melanoma patients, J. Clin. Invest. 125 (5) (2015) 2046–2058.
[6] A. Sucker, A. Paschen, Deciphering the genetic evolution of T-cell resistance in melanoma, Oncoimmunology 4 (5) (2015) e1005510.
[7] O. Susanto, S.E. Stewart, I. Voskoboinik, D. Brasacchio, M. Hagn, S. Ellis, S. Asquith, K.A. Sedelies, P.I. Bird, N.J. Waterhouse, J.A. Trapani, Mouse granzyme A induces a novel death with writhing morphology that is mechanistically distinct from granzyme B-induced apoptosis, Cell Death Differ. 20 (9) (2013) 1183–1193.
[8] S.H. Jang, M.S. Oh, H.I. Baek, K.C. Ha, J.Y. Lee, Y.S. Jang, Oral administration of silk peptide enhances the maturation and cytolytic activity of natural killer cells, Immune Netw 18 (5) (2018) e37.
[9] S.S. Metkar, B. Wang, M.L. Ebbs, J.H. Kim, Y.J. Lee, S.M. Raja, C.J. Froelich, Granzyme B activates procaspase-3 which signals a mitochondrial amplification loop for maximal apoptosis, J. Cell Biol. 160 (6) (2003) 875–885.
[10] M. Sebbagh, C. Renvoize, J. Hamelin, N. Riche, J. Bertoglio, J. Breard, Caspase-3-mediated cleavage of ROCK I induces MLC phosphorylation and apoptotic membrane blebbing, Nat. Cell Biol. 3 (4) (2001) 346–352.
[11] M.L. Coleman, E.A. Sahai, M. Yeo, M. Bosch, A. Dewar, M.F. Olson, Membrane blebbing during apoptosis results from caspase-mediated activation of ROCK I, Nat. Cell Biol. 3 (4) (2001) 339–345.
[12] J.C. Mills, N.L. Stone, J. Erhardt, R.N. Pittman, Apoptotic membrane blebbing is regulated by myosin light chain phosphorylation, J. Cell Biol. 140 (3) (1998) 627–636.
[13] B. Min, H. Choi, J.H. Her, M.Y. Jung, H.J. Kim, M.Y. Jung, E.K. Lee, S.Y. Cho, Y.K. Hwang, E.C. Shin, Optimization of large-scale expansion and cryopreservation of human natural killer cells for anti-tumor therapy, Immune Netw 18 (4) (2018) e31.
[14] K. Nakamura, N. Yoshikawa, Y. Yamaguchi, S. Kagota, K. Shinozuka, M. Kunitomo, Characterization of mouse melanoma cell lines by their mortal malignancy using an experimental metastatic model, Life Sci. 70 (7) (2002) 791–798.
[15] E.H. Seo, J.H. Namgung, C.S. Oh, S.H. Kim, S.H. Lee, Association of chemokines and chemokine receptor expression with monocytic-myeloid-derived suppressor cells during tumor progression, Immune Netw. 18 (3) (2018) e23.
[16] J.P. Medema, J. de Jong, L.T. Peltenburg, E.M. Verdegaal, A. Gorter, S.A. Bres, K.L. Franken, M. Hahne, J.P. Albar, C.J. Melief, R. Offringa, Blockade of the granzyme B/perforin pathway through overexpression of the serine protease inhibitor PI-9/SPI-6 constitutes a mechanism for immune escape by tumors, Proc. Natl. Acad. Sci. U. S. A. 98 (20) (2001) 11515–11520.
[17] M. Ray, D.R. Hostetter, C.R. Loeb, J. Simko, C.S. Craik, Inhibition of Granzyme B by PI-9 protects prostate cancer cells from apoptosis, Prostate 72 (8) (2012) 846–855.
[18] D.M. Benson Jr., C.E. Bakan, A. Mishra, C.C. Hofmeister, Y. Efebera, B. Becknell, R.A. Baiocchi, J. Zhang, J. Yu, M.K. Smith, C.N. Greenfield, P. Porcu, S.M. Devine, R. Rotem-Yehudar, G. Lozanski, J.C. Byrd, M.A. Caligiuri, The PD-1/PD-L1 axis modulates the natural killer cell versus multiple myeloma effect: a therapeutic target for CT-011, a novel monoclonal anti-PD-1 antibody, Blood 116 (13) (2010) 2286–2294.
[19] H. Saito, S. Takaya, T. Osaki, M. Ikeguchi, Increased apoptosis and elevated Fas expression in circulating natural killer cells in gastric cancer patients, Gastric Cancer 16 (4) (2013) 473–479.
[20] P. Van Damme, S. Maurer-Stroh, H. Hao, N. Colaert, E. Timmerman, F. Eisenhaber, J. Vandekerckhove, K. Gevaert, The substrate specificity profile of human granzyme A, Biol. Chem. 391 (8) (2010) 983–997.
[21] W. Xu, R. Mezencev, B. Kim, L. Wang, J. McDonald, T. Sulchek, Cell stiffness is a biomarker of the metastatic potential of ovarian cancer cells, PLoS One 7 (10) (2012) e46609.
[22] D.A. Fletcher, R.D. Mullins, Cell mechanics and the cytoskeleton, Nature 463 (7280) (2010) 485–492.
[23] M. Vicente-Manzanares, X. Ma, R.S. Adelstein, A.R. Horwitz, Non-muscle myosin II takes Centre stage in cell adhesion and migration, Nat. Rev. Mol. Cell Biol. 10 (11) (2009) 778–790.
[24] J.H. Wang, L. Zhang, S.T. Huang, J. Xu, Y. Zhou, X.J. Yu, R.Z. Luo, Z.S. Wen, W.H. Jia, M. Zheng, Expression and prognostic significance of MYL9 in esophageal squamous cell carcinoma, PLoS One 12 (4) (2017) e0175280.
[25] S. Medjkane, C. Perez-Sanchez, C. Gaggioli, E. Sahai, R. Treisman, Myocardin-related transcription factors and SRF are required for cytoskeletal dynamics and experimental metastasis, Nat. Cell Biol. 11 (3) (2009) 257–268.
[26] O. Holsken, M. Miller, A. Cerwenka, Exploiting natural killer cells for therapy of melanoma, J. Dtsch. Dermatol. Ges. 13 (1) (2015) 23–29.
[27] A. Gras Navarro, A.T. Bjorklund, M. Chekenya, Therapeutic potential and challenges of natural killer cells in treatment of solid tumors, Front. Immunol. 6 (2015) 202.